Clinical and Experimental Gastroenterology

Dovepress
Taylor & Francis Group

Open Access Full Text Article

ORIGINAL RESEARCH

Tumor-Stroma Ratio is a Critical Indicator of Peritoneal Metastasis in Gastric Cancer

Lin Zhong[1,*], Hongyun Huang[2,*], Dong Hou[1,*], Shihai Zhou[3], Yu Lin[4], Yue Yu[4], Jinhao Yu[1], Fanghai Han[5], Lang Xie[6]

[1]Department of Gastrointestinal Surgery, Sun Yat-Sen Memorial Hospital, Sun Yat-Sen University, Guangzhou, Guangdong, 510120, People's Republic of China; [2]Department of General Surgery, Peking Union Medical College Hospital, Chinese Academy of Medical Science and Peking Union Medical College, Beijing, 100010, People's Republic of China; [3]Department of Tumor Surgery, Zhongshan City People's Hospital, Zhongshan, Guangdong, 528403, People's Republic of China; [4]Department of Pathology, Zhujiang Hospital, Southern Medical University, Guangzhou, Guangdong, 510282, People's Republic of China; [5]Department of Gastrointestinal Surgery, Guangdong Second Provincial General Hospital, Guangzhou, Guangdong, 5181025, People's Republic of China; [6]Department of General surgery, Zhujiang Hospital, Southern Medical University, Guangzhou, Guangdong, 510282, People's Republic of China

*These authors contributed equally to this work

Correspondence: Lang Xie; Fanghai Han, Email langxiezj@hotmail.com; fh_han@163.com

Objective: This study aims to investigate the correlation between the tumor-stroma ratio (TSR) and peritoneal metastasis (PM) in gastric cancer (GC) and constructs a diagnostic model based on preoperative examination data.

Methods: To determine the feasibility of obtaining TSR in GC patients through preoperative examinations, the consistency of TSR between endoscopic biopsy tissues and postoperative histopathological tissues was evaluated. Additionally, the correlation between TSR and PM in GC was analyzed using Gene Expression Omnibus (GEO) datasets. To validate TSR's clinical potential in diagnosing PM, 640 GC patients from two medical centers were enrolled. A training cohort of 330 patients evaluated TSR and synchronous PM correlation, and a validation cohort of 310 patients was used. An additional cohort of 510 patients was established to investigate TSR and metachronous PM. A diagnostic model based on preoperative data was developed and a nomogram constructed.

Results: The TSR shows good consistency between endoscopic biopsy tissues and postoperative histopathological tissues. A significant correlation between TSR and PM was observed. The TSR-based model, combined with CA125, CA724 and Borrmann type, exhibited strong diagnostic effectiveness and considerable predictive efficacy, with an Area Under the Curve (AUC) of 0.85 in the training cohort, 0.73 in the external validation cohort, and 0.72 in the metachronous PM cohort.

Conclusion: The TSR emerges as a crucial marker for PM in GC, with the developed model, based on TSR and preoperative examination data, demonstrating substantial diagnostic and predictive capabilities.

Keywords: tumor-stroma ratio, peritoneal metastasis, gastric cancer, preoperative examinations, nomogram

Introduction

Gastric cancer (GC) ranks as one of the leading causes of cancer-related deaths globally. Peritoneal metastasis (PM) is a common complication in patients with advanced GC, often emerging as a prevalent form of postoperative recurrence.[1] PM can be categorized into synchronous and metachronous PM. It is estimated that 20–30% of patients present with PM at their initial diagnosis, and studies have demonstrated that 40–50% of patients with GC eventually develop PM.[2,3] Autopsy studies have revealed that up to 60% of GC-related deaths involve PM.[4]

Treating PM in GC remains a significant clinical challenge. Recent advances in treatment, such as neoadjuvant intraperitoneal therapies, immunotherapy, targeted therapies, and systemic chemotherapy, aim to improve patient outcomes.[5] However, these treatments often only control disease progression and alleviate symptoms, underscoring the importance of early diagnosis and appropriate therapeutic interventions for effective PM management in GC.[6]

Currently, computed tomography (CT) and staging laparoscopy are primary methods for diagnosing PM in GC patients. CT scans, however, show variable sensitivity (28–51%), particularly for detecting peritoneal metastases smaller

Received: 2 August 2024
Accepted: 9 January 2025
Published: 22 January 2025

than 5mm.7,[8] In contrast, staging laparoscopy, while invasive and potentially traumatic, boasts near 100% sensitivity.[9] Therefore, developing a simple, non-invasive, and sensitive diagnostic method for PM in GC is crucial. Existing diagnostic models, based on imaging data or tumor characteristics, are not entirely satisfactory. The tumor microenvironment (TME) is increasingly recognized for its role in cancer progression and metastasis.[10] A diagnostic model focusing on tumor stroma characteristics may offer new insights.

The tumor-stroma ratio (TSR) is a histological parameter that may provide valuable prognostic and diagnostic information, defined as the ratio between tumor cells and stromal components. TSR is generally associated with tumor progression, metastasis, response to chemotherapy, and survival.[11] It has been confirmed that the TSR is an important indicator of poor prognosis in GC. Our previous studies have confirmed that TSR is associated with metastatic nodules in GC.[12] However, the correlation between TSR and PM in GC has not been reported.

In the study, we investigate the correlation between TSR and PM in GC for the first time and construct a diagnostic model based on preoperative routine data.

Methods

TSR

The 4μm H&E-stained histological sections from all the patients were gathered for TSR analysis. Initially, a microscope offering a 5× field of view was employed to locate the deepest area of tumor cell infiltration. Furthermore, more than three distinct observation zones, each containing both tumor and stromal components and confirming the presence of surrounding tumor cells, were identified. TSR scoring was then performed using a microscope with a 10× field of view by calculating the stroma percentage in that field. Based on the TSR values, samples were categorized into two groups: a Low TSR group (<50%), representing a stroma-poor group, and a High TSR group (≥50%), indicating a stroma-rich group (Supplementary Figure 1).

The consistency of the evaluations conducted by the two pathologists was assessed using Cohen's kappa coefficient, which was 0.87 in this study, indicating a high level of agreement.

TSR Consistency

To validate the feasibility of TSR assessment through endoscopic tissue evaluation, paired endoscopic and postoperative pathological tissue biopsies from 35 patients were collected for TSR consistency analysis.

Public Database Data

The dataset GSE15081 was meticulously retrieved from the NCBI GEO database. The `xCell` R package was used to calculate the infiltration scores of Cancer-Associated Fibroblasts (CAFs). The `GraphPad Prism 9` software was utilized to analyze the difference between patients with PM and non-PM.

Retrospective Clinical Study Design

This retrospective study enrolled patients with GC treated at Zhujiang Hospital, Southern Medical University, between March 2014 and March 2021, and at Zhongshan City People's Hospital. In this study, PM was defined as a condition in which a pathological or imaging diagnosis confirms that GC has invaded and disseminated to the peritoneal surface, resulting in the formation of intraperitoneal metastatic lesions. To further investigate the correlation between TSR and metachronous PM, we combined patients from both centers who were initially diagnosed with GC and did not develop PM within three months post-surgery, creating a metachronous PM cohort (Figure 1). Due to the limitation of objective conditions, the peritoneal metastasis of patients was diagnosed according to the image data of Computed Tomography (CT) in the metachronous PM cohort.

Patients

Pertinent patient data were meticulously extracted from the databases of Zhujiang Hospital, Southern Medical University, and Zhongshan City People's Hospital. Inclusion and exclusion criteria were carefully implemented, as outlined below.

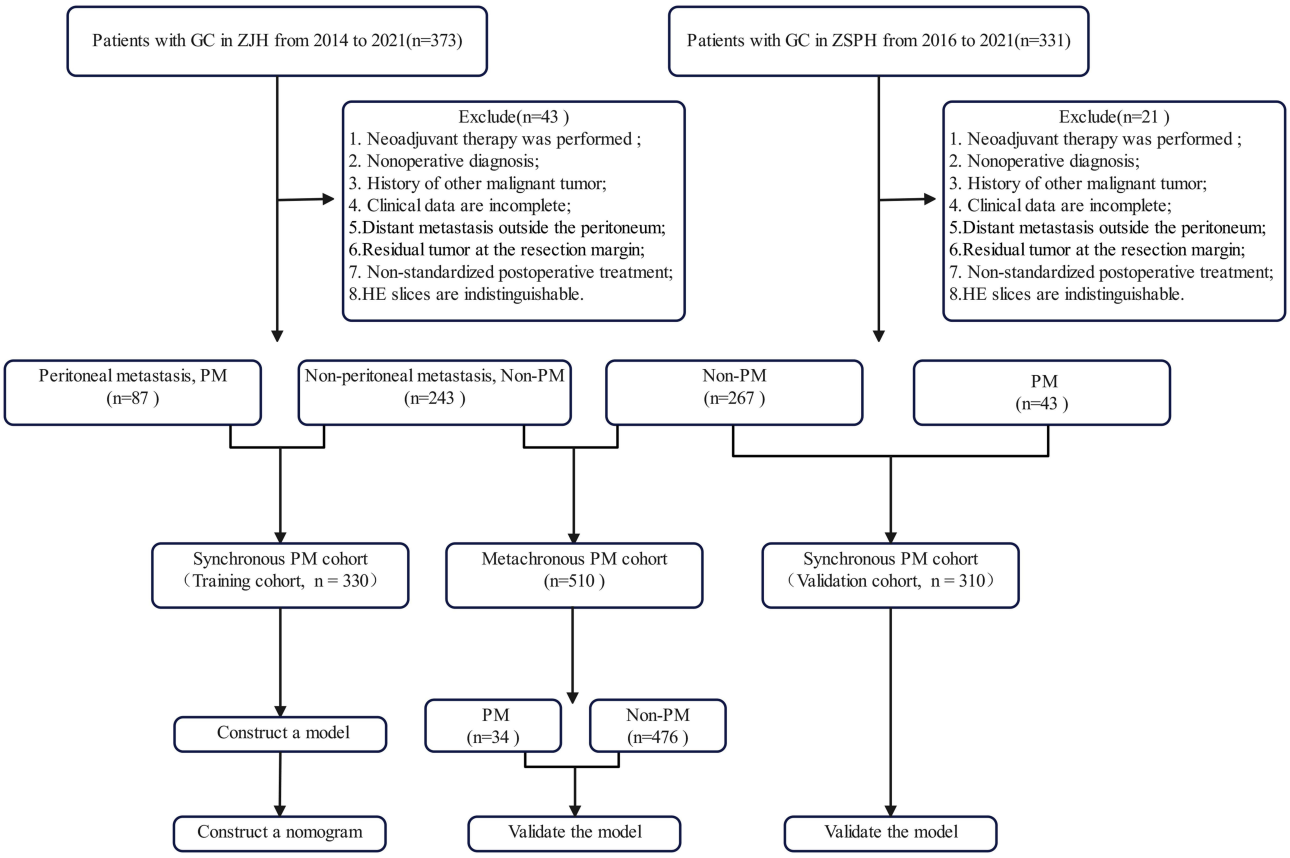

Figure 1 Flowchart of patient selection, exclusion, and grouping. The numbers in parentheses represent the number of patients.

Patient follow-up was primarily conducted via telephone inquiries, with additional information supplemented by reviews of outpatient case records. The follow-up ended in March 2021.

Inclusion Criteria

1. All patients must have received a pathological diagnosis confirming GC;
2. Every patient should have undergone surgical procedures, including stagging laparoscopy or radical gastrectomy;
3. All patients with PM of GC were confirmed through pathological examination;
4. Comprehensive follow-up data must be available for all study participants.

Exclusion Criteria

1. Patient missing relevant medical or personal information;
2. Patients who have previously undergone neoadjuvant therapy;
3. Patients with a history of other malignant tumors distinct from gastric cancer;
4. Postoperative pathological examination confirmed the presence of distant metastasis outside the peritoneum in patients;
5. Patients wherein residual tumor cells have been identified in the margins of the resected tissue upon postoperative pathology examination;
6. Patients whose postoperative treatment was not standardized;
7. Patients with incomplete data in HE stained histological sections.

https://doi.org/10.2147/CEG.S482377

Clinicopathology

Routine preoperative examination data were primarily collected, included variables such as sex, age, body mass index (BMI, BMI= weight/height ^2), white blood cell count (WBC, g/L), platelet count (PLT, g/L), albumin concentration (Alb, g/L), globulin concentration (Glo, g/L), albumin to globulin ratio (A/G), history of Helicobacter pylori infection (Hp), tumor site (0= entire stomach, 1 = cardia, 2 = stomach body, 3 = antrum), Borrmann type (0=type I and II; 1= type III and IV), maximum tumor diameter (Size, cm), alpha-fetoprotein levels (AFP, ng/mL), carcinoembryonic antigen (CEA, μg/L), cancer antigen 125 (CA125, kU/L), cancer antigen 153 (CA153, U/ mL), cancer antigen 199 (CA199, kU/ L), and cancer antigen 724 (CA724, U/mL).

Additionally, the T stage (staging according to the American Joint Committee on Cancer's 8th edition classification method determined), tumor differentiation rating Diff (0=undifferentiated, 1=low differentiation, 2 =medium differentiation, and 3 = high differentiation) and Her-2 (0= Negative, 1= Positive) were included.

Data Organization

Data were organized using R software, version 4.2.2. Acknowledging potential missing data during clinical data collection, the "mice" R package was employed to ensure data completeness and integrity (with less than 15% of the data imputed).

Statistical

All statistical analyses in this study were performed using R software, version 4.2.2.

The `tableone` R package was employed to create the data table The Shapiro–Wilk test was used to assess the normality of continuous variables, while the Mann–Whitney *U*-test was employed for comparisons between non-normal variables. Moreover, categorical variables and rank variables were compared by leveraging the $\chi 2$ and Fisher exact tests, respectively. We further used the `rms` R package for univariate and multivariate logistic regression analysis. To provide a comprehensive visualization of the analysis results, a forest plot was built through the `forestplot` R package. For the construction of the nomogram, several software packages such as `pROC`, `car`, and `rmda` came in handy. These were used to generate Receiver Operating Characteristic (ROC) curves, display the Area Under the Curve (AUC value), and produce a calibration curve, which were instrumental in verifying the model's effectiveness.

Statistical significance was assessed using two-tailed *t*-tests and was considered significant where $P < 0.05$ in the study.

Ethics

Ethical approval was granted by the Medical Ethics and System Committee of Zhujiang Hospital, Southern Medical University and Zhongshan City People's Hospital. All research procedures involving human participants in this study are in accordance with the Declaration of Helsinki. All patients provided informed consent for the collection of tissue specimens.

Results

TSR Shows Good Consistency in Endoscopic and Surgical Specimens

Effectively diagnosing the occurrence of PM in GC based on preoperative routine examinations holds significant clinical implications. TSR, an easy, fast, cost-neutral, and easily repeatable pathological parameter, has been proven to be associated with the prognosis of various cancers such as GC and colorectal cancer. Studies have shown good consistency in TSR assessment between biopsy and postoperative pathological tissues.[11,13] However, whether TSR based on preoperative endoscopic tissue can serve as a potential parameter for diagnosing PM requires further investigation.

We conducted a paired analysis of 35 patients to evaluate the consistency between endoscopic and postoperative TSR ratings. Endoscopy often fails to reach the deepest infiltrating tissues; thus, we collected tissues considered at the tumor's edge under endoscopic observation. We found a certain consistency in TSR scores between the two types of specimens (Figure 2a), with 1 out of 35 patients falling outside the Limits of Agreement (LoA) range, accounting for 2.85%, which

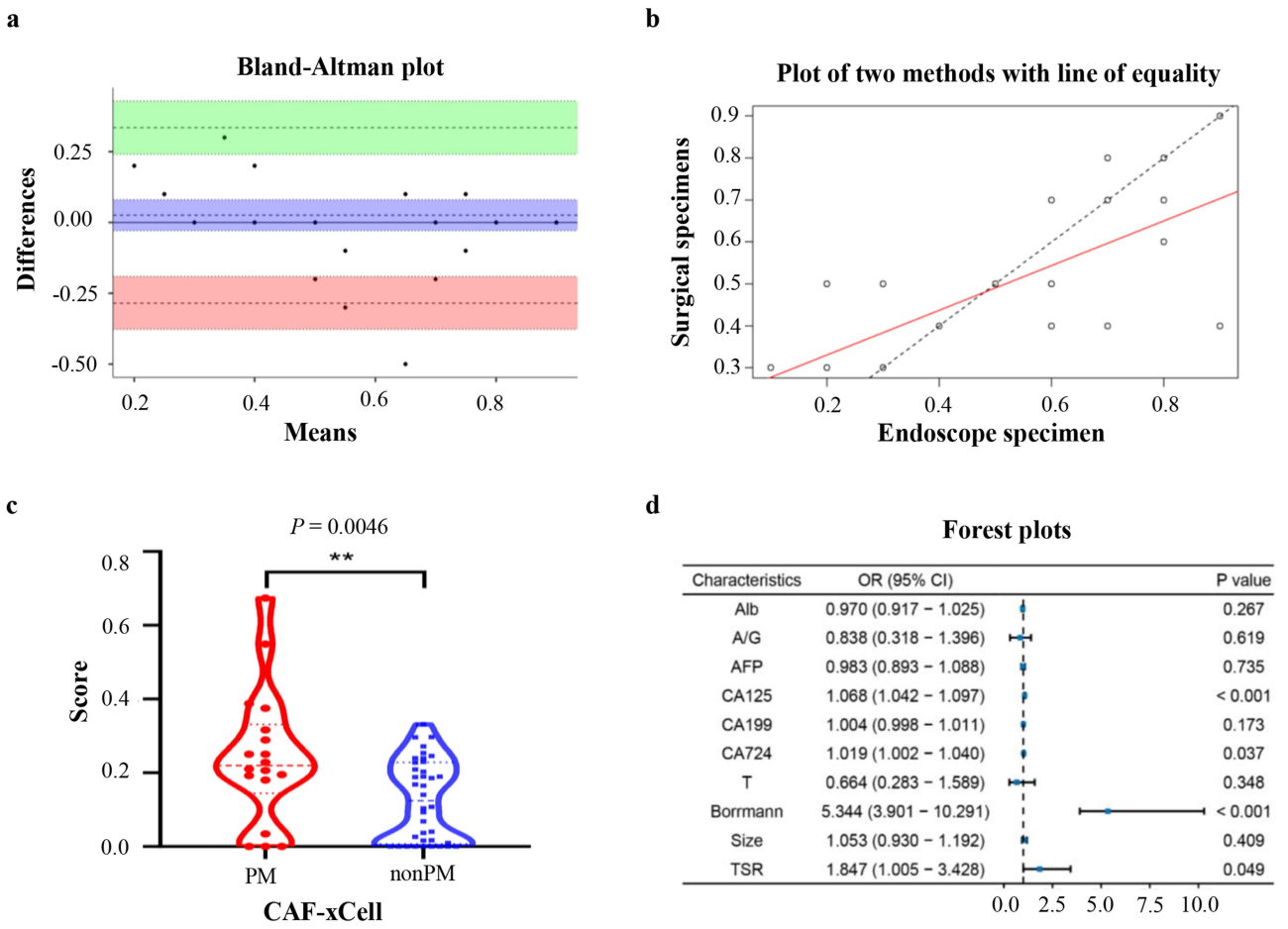

Figure 2 TSR based on routine preoperative exam parameters is a predictor of PM in GC. (**a** and **b**). Concordance of TSR in paired endoscopic and surgical specimens. (**a**) Bland-Altman plot drawn according to the TSR scores of paired endoscopic and surgical specimens; (**b**) Regression line drawn based on the TSR scores of paired endoscopic and surgical specimens. (**c**) CAF scoring for both the PM patients and non-PM patients. CAF scoring for both PM and non-PM patients. Patients were selected from the GSE15081 dataset for this purpose. The "Xcell" R package was utilized to conduct the CAF (Cancer-associated fibroblasts) scoring procedure. ***P* <0.01. (**d**) Describes the association between routine preoperative exam parameters and PM in GC by forest plot. The square in the plot represents the overall summary estimate of the analysis, and the width of the line segment indicates the 95% confidence interval (CI).

is less than 5%. The paired *t*-test *p* was 0.34, and the correlation coefficient of 0.79. However, the scatter plot shows that the consistency of the two scoring methods is not ideal (Figure 2b). When using 0.5 as the cutoff value to divide TSR into high and low groups, this consistency significantly improves (Table 1), where kappa is 0.706, AC1 (Agreement Coefficient 1) is 0.722, and the consistency is 85.7%. Therefore, endoscopic histopathological specimens can effectively be used for TSR ratings.

Table 1 Concordance of TSR in Paired Endoscopic and Surgical Specimens

n =35	TSR Low (SS)	TSR High (SS)	Kappa	AC1	Agreement %
			0.706	0.722	85.7%
TSR Low (ES)	18	2			
TSR High (ES)	3	12			

Notes: The Kappa and Gwet's AC1 statistics are interpreted as follows: <0.20, poor agreement; 0.21 to 0.40, fair agreement; 0.41 to 0.60, moderate agreement; 0.61 to 0.80, good agreement; 0.81 to 1.00, very good agreement.
Abbreviations: ES, Endoscope Specimens; SS, Surgical Specimens.

https://doi.org/10.2147/CEG.S482377

TSR is Associated with PM in GC

To objectively correlate tumor-associated stroma with peritoneal metastasis (PM) in gastric cancer (GC), we analyzed sequencing data of patients with PM obtained from the GEO database. This allowed us to examine the correlation between TSR and PM of GC at the mRNA level.

GSE15081, the chip with the largest number of sequencing samples and relatively complete information available from public databases, comprises a total of 141 samples, including 56 retrospective and 85 prospective samples. Cancer Associated Fibroblasts (CAFs), the primary components of the tumor-associated stroma, were scored using the `Xcell` R packages. The analysis revealed a significant statistical disparity between the two groups (P =0.0478), indicating that patients with PM had higher CAFs infiltration scores (Figure 2c).

In conclusion, the results reaffirm that tumor-associated stroma plays a key role in the regulating of PM in GC. These findings strengthen the association between TSR and PM in GC.

Clinicopathological Characteristics

To validate the clinical potential of TSR in diagnosing PM in GC, we enrolled GC patients from two independent medical centers. Based on the inclusion and exclusion criteria set forth, the study encompassed 640 participants. The study encompassed 640 participants, including 330 patients from Zhujiang Hospital, Southern Medical University, and 310 patients from Zhongshan City People's Hospital. Various parameters such as age, sex, BMI, WBC, Hb, PLT, Alb, Glo, gastrointestinal tumor marker, tumor location, tumor size, Borrmann type, T stage, differentiation degree, status of Her-2 and HP infection, and TSR grade were collected for analysis. All these parameters were acquired through preoperative hematological evaluation, computed tomography (CT) scan, gastroscopy, and pathological examination.

The patients from Zhujiang Hospital, Southern Medical University were comprised the model training cohort and were further classified into PM (87 patients) and non-PM groups (243 patients). The sex distribution was 67% male and 33% female, whereas the age distribution showed that 64% were less than 65 years old and 36% were 65 or above. Statistical analyses revealed significant differences between the two groups in metrics such as Alb, A/G, AFP, CEA, CA125, CA199, CA724, site, Size, T, Borrmann, Diff, and TSR (P <0.05). Among these parameters, Alb, CA125, CA724, Size, T, Borrmann, Diff, and TSR showed significant disparities (P <0.001) (Table 2).

For the study, patients from Zhongshan City People's Hospital were designated as the validation cohort. The cohort included 267 non-PM patients and 43 PM patients. The sex distribution was 68% male and 32% female, and the age breakdown was 63% under 65 years and 37% 65 or older. Significant differences in PLT, Alb, A/G, CA125, CA724, size, T, and TSR levels (P <0.05) were observed between the PM and non-PM groups. Notably, CA125, CA724, size, and T showed substantially between the cohorts (P <0.001) (Table 2).

In a concerted endeavor to validate the diagnostic model's efficacy in predicting PM in GC, patients from both centers who initially showed no signs of PM were collectively assigned to a metachronous PM cohort. This cohort consisted of 510 patients, with a sex distribution of 68% male and 32% female, and an age distribution of 63% under 65 and 37% 65 or older. In this cohort, age, size, T, Borrmann, Her-2, and TSR exhibited significant variation between PM and non-PM groups (P < 0.05) (Table 2).

Risk Factors Associated with PM of GC

To deepen our understanding of the risk factors influencing PM in GC, we carried out both univariate and multivariate logistic regression analyses. These analyses considered a range of variables within the training cohort. These variables include age, WBC, PLT, Alb, A/G, AFP, CEA, CA125, CA199, CA724, as well as Size, T, Diff, and TSR (Table 3). The univariate regression analysis revealed that the risk factors associated with PM included Alb (OR =0.923, P <0.001), A/G (OR =0.387, P =0.016), AFP (OR =1.140, P = 0.001), CA125 (OR =1.074, P <0.001), CA199 (OR =1.008, P =0.004), CA724 (OR =1.030, P =0.001), Size (OR =1.285, P <0.001), T (OR =3.125, P <0.001), Borrmann (OR = 18.251, P <0.001), and TSR (OR =2.717, P <0.001).

Table 2 Baseline Characteristics of Patients in the Training Cohort, Validation Cohort, and Metachronous PM Cohort

Characteristic		Training Cohort		*P*	Validation Cohort		*P*	Metachronous PM Cohort		*P*
	group	Non-PM N=243	PM N = 87		Non-PM N = 267	PM N = 43		Non-PM N = 476	PM N = 34	
Gender	Female	79 (33%)	30 (34%)	0.7	85 (32%)	15 (35%)	0.7	150 (32%)	14 (41%)	0.2
	Male	164 (67%)	57 (66%)		182 (68%)	28 (65%)		326 (68%)	20 (59%)	
Age	<65	154 (63%)	58 (67%)	0.6	167 (63%)	27 (63%)	>0.9	307 (64%)	14 (41%)	0.007
	≥65	89 (37%)	29 (33%)		100 (37%)	16 (37%)		169 (36%)	20 (59%)	
BMI		21.7 (19.4,24.0)	20.6 (19.2,23.1)	0.13	——	——	——	——	——	——
WBC		6.10 (4.97, 7.88)	6.82 (5.30, 9.06)	0.054	6.00 (4.94, 7.60)	6.71 (5.30, 7.85)	0.12	6.02 (4.92, 7.71)	6.39 (5.46, 8.09)	0.2
Hb		122 (96, 138)	111 (96, 133)	0.051	123 (96, 138)	112 (80, 134)	0.093	123 (96, 138)	116 (94, 134)	0.2
PLT		264 (210, 316)	267 (208, 358)	0.2	247 (202, 310)	307 (225, 368)	0.007	254 (205, 314)	250 (198, 307)	0.8
Alb		39.4 (35.3,42.9)	35.8 (32.0,41.3)	<0.001	39.7 (36.9, 42.0)	37.3 (33.9, 42.0)	0.044	39.7 (35.9, 42.6)	38.9 (35.6, 41.5)	0.4
Glo		26.9 (24.2,30.0)	27.1 (23.4,30.2)	>0.9	25.7 (23.0, 28.7)	26.8 (23.9, 30.1)	0.2	26.2 (23.5, 29.2)	25.8 (23.4, 29.0)	0.6
A/G		1.50 (1.30,1.70)	1.40 (1.10,1.60)	0.041	1.53 (1.38, 1.70)	1.41 (1.21, 1.62)	0.007	1.50 (1.30, 1.70)	1.51 (1.32, 1.70)	0.9
AFP		2.90 (2.32,3.66)	3.48 (2.29,5.53)	0.008	3 (2, 4)	3 (2, 6)	0.2	2.9 (2.0, 3.9)	2.8 (2.1, 3.9)	0.7
CEA		2 (1, 4)	3 (2, 6)	0.002	2.1 (1.1, 3.3)	2.2 (0.9, 4.4)	0.5	2.1 (1.2, 3.5)	2.6 (1.3, 5.5)	0.10
CA125		12 (9, 18)	26 (18, 41)	<0.001	10 (7, 15)	16 (9, 27)	<0.001	11 (8, 16)	11 (8, 18)	0.6
CA153		10.7 (7.6, 14.7)	11.1 (8.4, 13.3)	0.7	6.8 (5.6, 8.1)	7.0 (5.4, 11.0)	0.5	7.8 (6.2, 11.8)	9.0 (6.6, 14.0)	0.13
CA199		9 (6, 18)	16 (5, 40)	0.003	14 (8, 25)	18 (9, 78)	0.079	11 (6, 22)	10 (5, 26)	0.7
CA724		2 (1, 6)	6 (2, 17)	<0.001	4 (3, 7)	10 (4, 14)	<0.001	4 (2, 6)	5 (3, 13)	0.055
Site	0	3 (1.2%)	3 (3.4%)	0.034	0 (0%)	0 (0%)	0.2	3 (0.6%)	0 (0%)	0.7
	1	51 (21%)	20 (23%)		33 (12.4%)	9 (20.9%)		80 (16.8%)	4 (11.8%)	
	2	43 (17.7%)	25 (28.7%)		17 (6.4%)	4 (9.3%)		57 (12%)	3 (8.8%)	
	3	146 (60.1%)	39 (44.9%)		217 (81.2%)	30 (69.8%)		336 (70.6%)	27 (79.4%)	
Size		4.00 (2.50,6.00)	6.00 (4.00,8.00)	<0.001	3.50 (2.00, 4.50)	5.30 (3.88, 6.59)	<0.001	3.50 (2.00, 5.00)	4.00 (4.00, 6.00)	0.002
Hp	0	189 (78%)	60 (69%)	0.10	——	——	——	——	——	——
	1	54 (22%)	27 (31%)		——	——	——	——	——	——
T	T1	52 (21.4%)	11 (12.7%)	<0.001	61 (22.8%)	2 (4.7%)	<0.001	111 (23.3%)	2 (5.9%)	<0.001
	T2	29 (11.9%)	1 (1.1%)		39 (14.6%)	1 (2.3%)		66 (13.9%)	2 (5.9%)	
	T3	19 (7.8%)	1 (1.1%)		41 (15.4%)	3 (7.0%)		60 (12.6%)	0 (0%)	
	T4	143 (58.9%)	74 (85.1%)		120 (45%)	33 (76.7%)		233 (48.9%)	30 (88.2%)	
	Tis	0	0		6 (2.2%)	4 (9.3%)		6 (1.3%)	0 (0%)	
Borrmann	1	21 (8.6%)	1 (1.1%)	<0.001	4 (1.5%)	0 (0%)	0.4	25 (5.3%)	0 (0%)	0.008

(*Continued*)

https://doi.org/10.2147/CEG.S482377

Table 2 (Continued).

Characteristic		Training Cohort		*P*	Validation Cohort		*P*	Metachronous PM Cohort		*P*
	group	Non-PM N=243	PM N = 87		Non-PM N = 267	PM N = 43		Non-PM N = 476	PM N = 34	
	2	52 (21%)	2 (2.3%)		30 (11%)	2 (4.7%)		82 (17%)	0 (0%)	
	3	168 (69%)	71 (82%)		233 (87%)	41 (95%)		367 (77%)	34 (100%)	
	4	2 (0.8%)	13 (15%)		0 (0%)	0 (0%)		2 (0.4%)	0 (0%)	
Diff	0	10 (4.1%)	1 (1.1%)	<0.001	0 (0%)	0 (0%)	0.5	8 (1.7%)	2 (5.9%)	0.064
	1	5 (2.1%)	0 (0%)		191 (71.5%)	32 (74%)		178 (37.4%)	18 (52.9%)	
	2	62 (25.5%)	7 (8.1%)		64 (24%)	11 (26%)		121 (25.4%)	5 (14.7%)	
	3	166 (68.3%)	79 (90.8%)		12 (4.5%)	0 (0%)		169 (35.5%)	9 (26.5%)	
Her-2	0	178 (73%)	67 (77%)	0.5	159 (60%)	30 (70%)	0.2	320 (67%)	17 (50%)	0.040
	1	65 (27%)	20 (23%)		108 (40%)	13 (30%)		156 (33%)	17 (50%)	
TSR	Low	147 (60%)	31 (36%)	<0.001	147 (55%)	14 (33%)	0.006	280 (59%)	14 (41%)	0.044
	High	96 (40%)	56 (64%)		120 (45%)	29 (67%)		196 (41%)	20 (59%)	

Notes: Site (0=entire stomach, 1=cardia, 2=stomach body, 3=antrum); Borrmann type (0=type I and II; 1= type III and IV), "Diff" (0=undifferentiated, 1=low differentiation, 2 =medium differentiation, 3 = high differentiation); Her-2 (0= Negative, 1= Positive); n (%); Median (IQR); Pearson's Chi-squared test; Wilcoxon rank sum test; Fisher's exact test.

https://doi.org/10.2147/CEG.S482377

Table 3 Univariate and Multivariate Regression Analysis in the Training Cohort

Characteristics	Total(N)	Univariate Analysis		Multivariate Analysis	
		Odds Ratio (95% CI)	*P* value	Odds Ratio (95% CI)	*P* value
Age	330				
<65	212	Reference			
≥65	118	0.915 (0.548–1.547)	0.737		
WBC	330	0.910 (0.813–1.006)	0.054		
PLT	330	1.002 (1.000–1.005)	0.056		
Alb	330	0.923 (0.885–0.960)	< 0.001	0.970 (0.917–1.025)	0.267
A/G	330	0.387 (0.176–0.817)	0.016	0.838 (0.318–1.396)	0.619
AFP	330	1.140 (1.057–1.244)	0.001	0.983 (0.893–1.088)	0.735
CA125	330	1.074 (1.053–1.097)	< 0.001	1.068 (1.042–1.097)	< 0.001
CA199	330	1.008 (1.003–1.015)	0.004	1.004 (0.998–1.011)	0.173
CA724	330	1.030 (1.013–1.050)	0.001	1.019 (1.002–1.040)	0.037
Size	330	1.285 (1.171–1.417)	< 0.001	1.053 (0.930–1.192)	0.41
T	330				
T1+T2	93	Reference		Reference	
T3+T4	237	3.125 (1.659–6.343)	< 0.001	0.664 (0.283–1.589)	0.348
Borrmann	330				
0	75	Reference		Reference	
1	255	18.251 (5.550–112.678)	< 0.001	5.344 (3.901–10.291)	< 0.001
Diff	330				
0	11	Reference			
1	5	0.000 (0.000–14,036.253)	0.984		
2	69	1.129 (0.173–22.269)	0.914		
3	245	4.759 (0.888–88.101)	0.140		
Her-2	330				
0	245	Reference			
1	85	0.817 (0.452–1.433)	0.492		
TSR	330				
Low	178	Reference		Reference	
High	152	2.717 (1.642–4.562)	< 0.001	1.847 (1.005–3.428)	0.049

Notes: Borrmann type (0=type I and II; 1= type III and IV), "Diff" (0=undifferentiated, 1=low differentiation, 2 =medium differentiation, and 3 = high differentiation), Her-2 (0= Negative, 1= Positive).
Abbreviations: OR, odds ratio; CI, confidence interval.

To enhance the clarity and visualization of these risk factors, Forest plots were created based on the findings from the multivariate logistic regression analysis. As depicted in Figure 2d, CA125, CA724, Borrmann, and TSR are unequivocally identified as substantial risk factors.

Diagnostic Model Construction Based on TSR and Preoperative Data

Based on the findings detailed above, it is evident that CA125, CA724, Borrmann, and TSR are critical risk factors for PM in GC. Following a comprehensive analysis, we constructed a risk score model for all patients, resulting in the following predictive equation:

Risk Score = 0.0688 * CA125 + 0.0231 * CA724 +2.7303 * Borrmann+ 0.6150*(TSR≥50%)-5.4622.

Consequently, the probability of PM can be calculated by the formula:

Probability of PM = 1 / (1 + e^ (- Risk Score))

To ensure ease of clinical application, we have designed a Nomogram model to provide a visual interpretation of these results. As shown in Figure 3a, the impact of variables on PM in our nomogram is represented by the length of the corresponding lines and their associated scores. Each patient receives individualized scores based on relevant risk factors. The total score for all variables determines the probability of PM in GC patients.

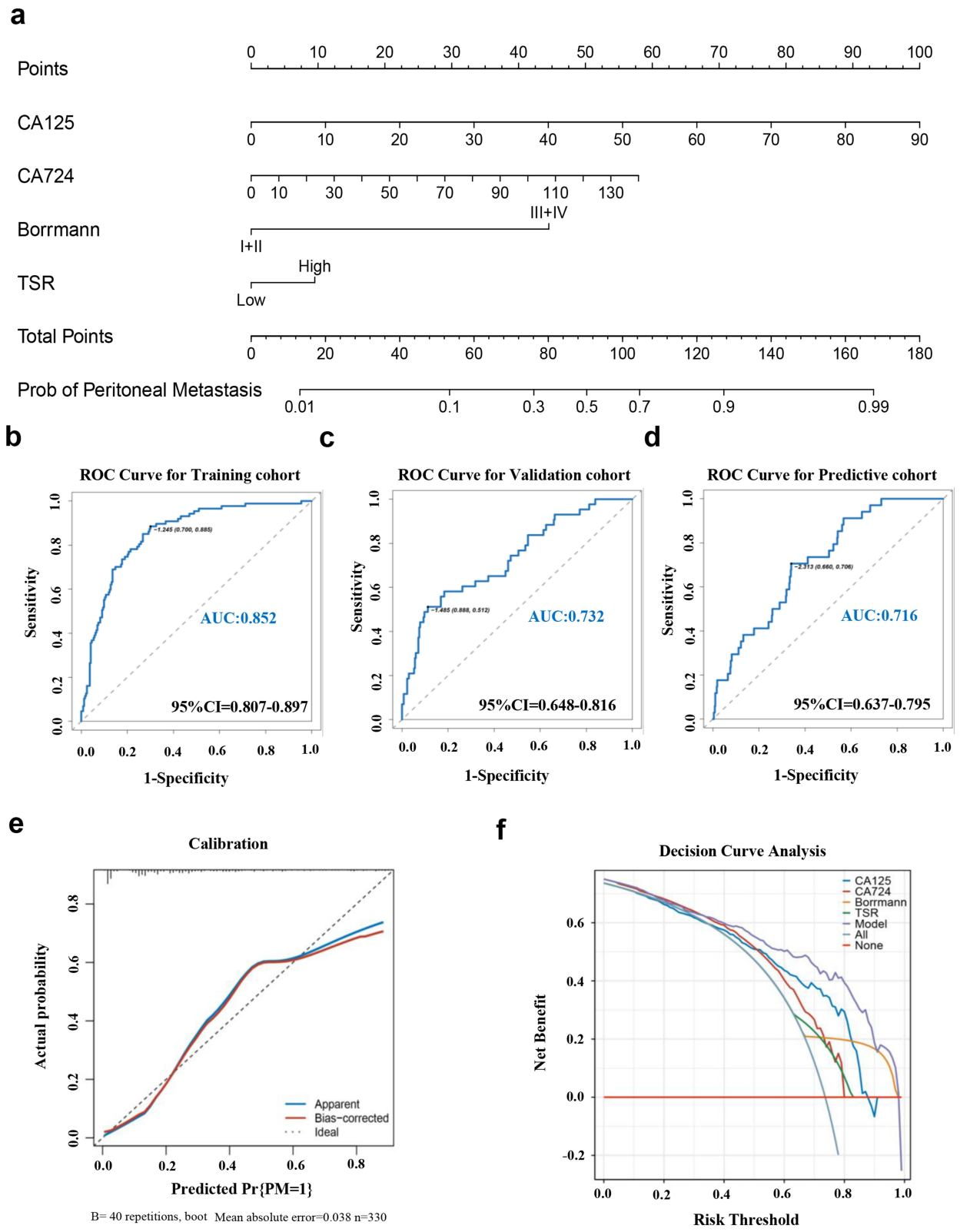

Figure 3 Model performance and validation. (**a**) Competing-risk nomogram incorporating TSR, CA724, CA125 and Borrmann; (**b**) The diagnostic performance of the model in the training cohort; (**c**) The diagnostic performance of the model in the external validation cohort; (**d**) The diagnostic performance of the model in the prediction cohort; (**e**) Calibration curve of the model in the training cohort. The blue line represents the performance of the nomogram, while the red line corrects any bias in the nomogram. The dotted line represents the reference line where the ideal nomogram is located; (**f**) Decision curve analysis demonstrating the model's decision benefit in practical clinical applications. The x-axis represents the threshold probability. The y-axis measures net benefits.

Model Performance and Validation

Because the endpoint event of the model is a categorical variable, the Consistency Index (C-index), which is equivalent to the AUC, achieved a value of 0.852 (95% CI: 0.807–0.897) and is used to diagnose PM in the training cohort, as shown in Figure 3b. Notably, this model also demonstrated good discrimination in the validation cohort, with a C-index of 0.732 (95% CI:0.648–0.816), as depicted in Figure 3c. Furthermore, the C-index calculated based on the metachronous PM cohort was 0.72, with a 95% CI of 0.637–0.795, as presented in Figure 3d. The calibration curve reveals that in the training cohort, the Mean Absolute Error (MAE) is 0.038, in the external validation cohort, the MAE is 0.034, and in the metachronous PM cohort, the MAE is 0.006. This indicates that the predictive model has a small average difference between its predictions and the actual observed values, demonstrating high predictive accuracy. However, in the metachronous PM cohort, the long-term predictive performance of the model is somewhat lacking due to the influence of time factors (Figure 3e). As a holistic evaluation, the diagnostic efficacy of the model is acceptable, but its prediction of PM recurrence in GC is less than satisfactory. Decision curve analysis (DCA) demonstrated that a treatment strategy guided by the model's diagnosis proved more advantageous compared to approaches based on other indices, indicating the model's substantial clinical utility in diagnosing PM in gastric cancer GC (Figure 3f).

Discussion

The peritoneum is the most common site of metastasis for GC, with about one-third of patients presenting with PM at the time of initial diagnosis.[14] Patients with PM are highly prone to complications such as intestinal obstruction, ascites, and cachexia. These hard-to-control complications often serve as significant factors leading to death. Effectively controlling the progression of PM not only improves the patient's quality of life but also significantly extends their survival time.[15] The cause of death in approximately 60% of advanced GC patients is attributed to PM.[16] Since the 1980s, CRS (Cytoreductive Surgery) / HIPEC (Hyperthermic Intraperitoneal Chemotherapy) has been recommended for treating PM in GC; however, the application of HIPEC remains a major controversy.[15] Multiple studies confirm that the completeness of CRS and a low peritoneal carcinomatosis index (PCI) are important factors affecting prognosis.[5] The neoadjuvant intraperitoneal chemotherapy and neoadjuvant HIPEC can effectively reduce the PCI, increasing the possibility of complete CRS.[17,18] With comprehensive treatment, the overall survival rate of GC patients with PM has significantly improved, with approximately 10% of patients surviving for more than 10 years.[6] The accurate diagnosis of GC with PM is not only a key factor in formulating treatment strategies but also crucial for improving the patient's prognosis.

Traditional imaging examinations, such as CT scans, cannot diagnose PM both timely and accurately, with CT scans showing only a sensitivity of 28% to 51%.[7,8] For this reason, diagnostic laparoscopy and peritoneal lavage fluid examination have gradually become the most important methods for diagnosing PM in GC.[19,20] However, both are invasive procedures performed under anesthesia, often posing risks to both the psychological and physiological health of patients. Therefore, a timely, accurate, and minimally traumatic diagnosis of PM in GC holds significant clinical importance.

In recent years, there has been a growing trend of applying multi-omics techniques in the diagnosis of PM in GC. This advanced technology significantly enhances both diagnostic precision and predictive capabilities. Lee IS et al revealed key findings through transcriptome sequencing analysis. A predictive model was constructed, which includes ZBTB1, CAVIN2, CHCHD3, LTBP3, SLITRK6, and STT3B, and can effectively predict the occurrence of PM in GC (AUC=0.72).[21] Liu S et al have effectively enhanced the diagnostic performance of CT in detecting elusive peritoneal metastatic nodules using radiomics (AUC=0.618–0.658).[22] Yanyan Chen et al have developed a predictive model leveraging proteomics analysis, which includes DUOXA2, ITGA7, LIMS1, MSRB3, PLCB1, RAB6B, SEMA3C, SMTN, TADA1, and TBC1D14. This model can effectively predict the occurrence of PM in GC (AUC=0.83).[23] Although the results of these studies are admirable, there are still clearly identified areas for improvement, such as additional economic pressure on patients, insufficient comprehensiveness of biomarkers, patient cohorts not meeting necessary size requirements, and a lack of multi-center validation, which hinders broader clinical applicability.

Currently, most research still focuses on the characteristics of tumors. However, the tumor microenvironment (TME) is beginning to garner increasing attention in the scientific community. Several proficient teams have orchestrated successful predictions for PM, leveraging distinct features such as metabolism,[24] immunity[25] and collagen inherent[26] within the TME. For instance, Dexin Chen et al found that a high collagen signature is a risk factor for PM in GC,[26] the predictive model based on this delivers an area under the receiver operating characteristic curve (AUROC) of 0.825, substantiated by external validation at 0.776. The TME is a critical factor in tumor metastasis,[27] consists of tumor cells, stromal cells, immune cells, chemokines, cytokines, and others. The tumor-associated stroma is an important part of the TME. Investigating the correlation between the TME and the PM of GC is of great necessity.

TSR, as an easy, fast, cost-neutral, and easily repeatable pathological parameter, can intuitively describe the relationship between tumor cells and tumor-associated stroma. Several studies have conclusively established that TSR serves as an independent prognostic marker for a variety of tumors. Scoring criteria have been established for breast cancer, and colorectal cancer.[28] Many studies have identified TSR as an independent prognostic indicator for GC. Reinforcing this conclusion, our previous studies have unveiled that stroma-rich metastatic nodules serve as independent determinants of poor prognosis in GC.[12] By integrating TSR with the traditional TNM staging system, it has been demonstrated that the predictive accuracy regarding patient outcomes in GC can be considerably improved.[29] In this study, we further discovered that TSR is closely related to the occurrence of PM in GC, serving as a potentially important indicator for diagnosing PM in GC.

Based on the results of univariate regression analysis, multivariate logistic regression was performed. The outcome of this multivariate analysis revealed that CA125 (OR =1.067, $P < 0.001$), CA724 (OR =1.019, P =0.037), Borrmann (OR =5.344, $P < 0.001$), and TSR (OR= 1.847, P =0.049) are significantly associations with PM in GC. We developed a diagnostic model utilizing CA125, CA724, Borrmann, and TSR as variables, which can effectively predict the occurrence of PM in GC (AUC= 0.852, external validation = 0.732). CA125 and CA724, frequently used as tumor markers in assessing digestive tract malignancies, can be evaluated through hematological testing. Information regarding the Borrmann type can be acquired through endoscopy. In this study, while we employed tissue specimens for TSR scoring, we confirmed that the TSR grading of tissues obtained via endoscopy is highly consistent with postoperative histopathology, as indicated by a Kappa value of 0.706, an AC1 of 0.722, and an agreement rate of 85.7%. Concurrently, it has been substantiated that there is substantial concordance between the TSR of biopsy tissues and surgical tissue specimens in laryngeal cancer and tongue cancer, with AC1 values of 0.796 and 0.769, respectively.[11,13] Therefore, we believe TSR can be effectively procured via gastric endoscopy biopsy. Additionally, the stroma-epithelial gene characteristic ratio in colorectal cancer patients can be described by liquid biopsy. This parameter is highly consistent with TSR and serves as an effective prognostic indicator for colorectal cancer patients.[28] Thus, hematological analysis could potentially serve as an efficient approach for obtaining the TSR. Consequently, all essential parameters required for the model can be conveniently obtained from routine preoperative assessments.

The model developed in this study exhibits an overall sensitivity, specificity, and accuracy of 88.5%, 70.0%, and 79.3% respectively, making it a robust tool for clinicians while formulating treatment strategies. What`s more, the model demonstrates good predictive performance for metachronous PM, offering guidance for the treatment and follow-up of postoperative GC patients.

This study acknowledges several limitations that merit attention. First, our data were derived solely from two medical centers, thereby requiring further verification with more external data, specifically from Western countries. Second, due to the retrospective nature of our analysis, unavoidable discrepancies may crop up when compared to prospective research; hence, corroborating these findings with future prospective studies becomes crucial. Third, none of the participants in this investigation had undergone neoadjuvant radiotherapy or chemotherapy, which could alter the morphology of the H&E sections. Thus, we should emphasize the need for added scrutiny when considering the applicability of this model to patients who have previously received neoadjuvant radiotherapy or chemotherapy. Fourth, the scope of preoperative examination parameters encompassed in this study was somewhat limited. A more profound exploration into the deeper implications of preoperative examination data via omics techniques, and their application in diagnosing PM in gastric cancer GC, holds substantial significance. This is also an area of research that we are currently undertaking. Lastly, the series of key genes we identified calls for robust affirmation through meticulous in vivo and in vitro experimentation.

Conclusion

In conclusion, this study is the first to indicate that the TSR is a critical indicator of PM in GC. We developed a diagnostic model based on preoperative routine examination results, which has shown promising diagnostic efficacy and provides a valuable reference for formulating clinical treatment strategies. Thus, our findings provide a crucial theoretical basis for optimizing diagnostic approaches of PM in GC.

Abbreviations

TSR, Tumor-stroma ratio; PM, Peritoneal metastasis; GC, Gastric cancer; AUC, Area Under the Curve; CT, computed tomography; TME, Tumor microenvironment; CAFs, Cancer-Associated Fibroblasts; MAE, Mean Absolute Error; DCA, Decision curve analysis; AUROC, Area under the receiver operating characteristic curve; OR, Odds ratio; CI, Confidence interval.

Data Sharing Statement

The datasets generated and/or analyzed related to this publication are available from the corresponding author upon reasonable request.

Ethics Approval and Informed Consent

Ethical approval was granted by the Medical Ethics and System Committee of Zhujiang Hospital, Southern Medical University and Zhongshan City People's Hospital (2024-KY-417-01). All research procedures involving human participants in this study are in accordance with the Declaration of Helsinki.

Consent for Publication

We acknowledge that we have reviewed and agree to the journal's editorial policies and guidelines. We confirm that we have obtained and can provide copies of signed consent forms from all individuals whose images, recordings, or other personal data are included in the manuscript, as required by the journal's editorial office.

Author Contributions

All authors made a significant contribution to the work reported, whether that is in the conception, study design, execution, acquisition of data, analysis and interpretation, or in all these areas; took part in drafting, revising or critically reviewing the article; gave final approval of the version to be published; have agreed on the journal to which the article has been submitted; and agree to be accountable for all aspects of the work.

Funding

This research was supported by China Postdoctoral Science Foundation (2022M723656), Guangzhou Key Project Research and Development Program(No. 202206080007).

Disclosure

The authors declare that they have no conflicts of interest in this work.

References

1. Gwee YX, Chia DKA, So J, et al. Integration of genomic biology into therapeutic strategies of gastric cancer peritoneal metastasis. *J Clin Oncol*. 2022;40(24):2830. doi:10.1200/JCO.21.02745
2. Gotze TO, Piso P, Lorenzen S, et al. Preventive HIPEC in combination with perioperative FLOT versus FLOT alone for resectable diffuse type gastric and gastroesophageal junction type II/III adenocarcinoma - the Phase III "PREVENT"- (FLOT9) trial of the AIO /CAOGI /ACO. *BMC Cancer*. 2021;21(1):1158. doi:10.1186/s12885-021-08872-8
3. Gong X, Hou D, Zhou S, et al. FMO family may serve as novel marker and potential therapeutic target for the peritoneal metastasis in gastric cancer. *Front Oncol*. 2023;13:1144775. doi:10.3389/fonc.2023.1144775
4. Montori G, Coccolini F, Ceresoli M, et al. The treatment of peritoneal carcinomatosis in advanced gastric cancer: state of the art. *Int J Surg Oncol*. 2014;2014:912418. doi:10.1155/2014/912418

5. Bonnot PE, Piessen G, Kepenekian V, et al. Cytoreductive surgery with or without hyperthermic intraperitoneal chemotherapy for gastric cancer with peritoneal metastases (CYTO-CHIP study): a propensity score analysis. *J Clin Oncol*. 2019;37(23):2028–2040. doi:10.1200/JCO.18.01688
6. Yonemura Y, Prabhu A, Sako S, et al. Long term survival after cytoreductive surgery combined with perioperative chemotherapy in gastric cancer patients with peritoneal metastasis. *Cancers*. 2020;12(1):116. doi:10.3390/cancers12010116
7. Yajima K, Kanda T, Ohashi M, et al. Clinical and diagnostic significance of preoperative computed tomography findings of ascites in patients with advanced gastric cancer. *Am J Surg*. 2006;192(2):185–190. doi:10.1016/j.amjsurg.2006.05.007
8. Kim SJ, Kim HH, Kim YH, et al. Peritoneal metastasis: detection with 16- or 64-detector row CT in patients undergoing surgery for gastric cancer. *Radiology*. 2009;253(2):407–415. doi:10.1148/radiol.2532082272
9. Fujimura T, Kinami S, Ninomiya I, et al. Diagnostic laparoscopy, serum CA125, and peritoneal metastasis in gastric cancer. *Endoscopy*. 2002;34 (7):569–574. doi:10.1055/s-2002-33228
10. Valkenburg KC, de Groot AE, Pienta KJ. Targeting the tumour stroma to improve cancer therapy. *Nat Rev Clin Oncol*. 2018;15(6):366–381. doi:10.1038/s41571-018-0007-1
11. Alessandrini L, Ferrari M, Taboni S, et al. Tumor-stroma ratio, neoangiogenesis and prognosis in laryngeal carcinoma. A pilot study on preoperative biopsies and matched surgical specimens. *Oral Oncol*. 2022;132:105982. doi:10.1016/j.oraloncology.2022.105982
12. Huang J, Yang B, Tan J, et al. Gastric cancer nodal tumour-stroma ratios influence prognosis. *Br J Surg*. 2020;107(13):1713–1718. doi:10.1002/bjs.12054
13. Bello IO, Wennerstrand PM, Suleymanova I, et al. Biopsy quality is essential for preoperative prognostication in oral tongue cancer. *APMIS*. 2021;129(3):118–127. doi:10.1111/apm.13104
14. Koemans WJ, Lurvink RJ, Grootscholten C, Verhoeven RHA, de Hingh IH, van Sandick JW. Synchronous peritoneal metastases of gastric cancer origin: incidence, treatment and survival of a nationwide Dutch cohort. *Gastric Cancer*. 2021;24(4):800–809. doi:10.1007/s10120-021-01160-1
15. Foster JM, Zhang C, Rehman S, Sharma P, Alexander HR. The contemporary management of peritoneal metastasis: a journey from the cold past of treatment futility to a warm present and a bright future. *CA Cancer J Clin*. 2023;73(1):49–71. doi:10.3322/caac.21749
16. Yang XJ, Huang CQ, Suo T, et al. Cytoreductive surgery and hyperthermic intraperitoneal chemotherapy improves survival of patients with peritoneal carcinomatosis from gastric cancer: final results of a phase III randomized clinical trial. *Ann Surg Oncol*. 2011;18(6):1575–1581. doi:10.1245/s10434-011-1631-5
17. Badgwell B, Blum M, Das P, et al. Phase II trial of laparoscopic hyperthermic intraperitoneal chemoperfusion for peritoneal carcinomatosis or positive peritoneal cytology in patients with gastric adenocarcinoma. *Ann Surg Oncol*. 2017;24(11):3338–3344. doi:10.1245/s10434-017-6047-4
18. Yonemura Y, Elnemr A, Endou Y, et al. Effects of neoadjuvant intraperitoneal/systemic chemotherapy (bidirectional chemotherapy) for the treatment of patients with peritoneal metastasis from gastric cancer. *Int J Surg Oncol*. 2012;2012:148420. doi:10.1155/2012/148420
19. Sato Y, Mizusawa J, Katayama H, et al. Diagnosis of invasion depth in resectable advanced gastric cancer for neoadjuvant chemotherapy: an exploratory analysis of Japan clinical oncology group study: JCOG1302A. *Eur J Surg Oncol*. 2020;46(6):1074–1079. doi:10.1016/j.ejso.2020.02.038
20. Allen CJ, Blumenthaler AN, Das P, et al. Staging laparoscopy and peritoneal cytology in patients with early stage gastric adenocarcinoma. *World J Surg Oncol*. 2020;18(1):39. doi:10.1186/s12957-020-01813-y
21. Lee IS, Lee H, Hur H, et al. Transcriptomic profiling identifies a risk stratification signature for predicting peritoneal recurrence and micrometastasis in gastric cancer. *Clin Cancer Res*. 2021;27(8):2292–2300. doi:10.1158/1078-0432.CCR-20-3835
22. Liu S, He J, Liu S, et al. Radiomics analysis using contrast-enhanced CT for preoperative prediction of occult peritoneal metastasis in advanced gastric cancer. *Eur Radiol*. 2020;30(1):239–246. doi:10.1007/s00330-019-06368-5
23. Chen Y, Cai G, Jiang J, et al. Proteomic profiling of gastric cancer with peritoneal metastasis identifies a protein signature associated with immune microenvironment and patient outcome. *Gastric Cancer*. 2023;26(4):504–516. doi:10.1007/s10120-023-01379-0
24. Kaji S, Irino T, Kusuhara M, et al. Metabolomic profiling of gastric cancer tissues identified potential biomarkers for predicting peritoneal recurrence. *Gastric Cancer*. 2020;23(5):874–883. doi:10.1007/s10120-020-01065-5
25. Zhang C, Li D, Yu R, et al. Immune landscape of gastric carcinoma tumor microenvironment identifies a peritoneal relapse relevant immune signature. *Front Immunol*. 2021;12:651033. doi:10.3389/fimmu.2021.651033
26. Chen D, Liu Z, Liu W, et al. Predicting postoperative peritoneal metastasis in gastric cancer with serosal invasion using a collagen nomogram. *Nat Commun*. 2021;12(1):179. doi:10.1038/s41467-020-20429-0
27. Entenberg D, Oktay MH, Condeelis JS. Intravital imaging to study cancer progression and metastasis. *Nat Rev Cancer*. 2023;23(1):25–42. doi:10.1038/s41568-022-00527-5
28. Ravensbergen CJ, Kuruc M, Polack M, et al. The stroma liquid biopsy panel contains a stromal-epithelial gene signature ratio that is associated with the histologic tumor-stroma ratio and predicts survival in colon cancer. *Cancers*. 2021;14(1):163. doi:10.3390/cancers14010163
29. Peng C, Liu J, Yang G, Li Y. The tumor-stromal ratio as a strong prognosticator for advanced gastric cancer patients: proposal of a new TSNM staging system. *J Gastroenterol*. 2018;53(5):606–617. doi:10.1007/s00535-017-1379-1